HHS Public Access

Author manuscript

Science. Author manuscript; available in PMC 2017 June 17.

Published in final edited form as:

Science. 2016 June 17; 352(6292): aad1210. doi:10.1126/science.aad1210.

T helper 1 immunity requires complement-driven NLRP3 inflammasome activity in CD4+ T cells

Giuseppina Arbore[#1], **Erin E. West**[#2], **Rosanne Spolski**[2], **Avril A. B. Robertson**[3], **Andreas Klos**[4], **Claudia Rheinheimer**[4], **Pavel Dutow**[4], **Trent M. Woodruff**[3], **Zu Xi Yu**[5], **Luke A. O'Neill**[6], **Rebecca C. Coll**[3], **Alan Sher**[7], **Warren J. Leonard**[2], **Jörg Köhl**[8,9], **Pete Monk**[10], **Matthew A. Cooper**[3], **Matthew Arno**[11], **Behdad Afzali**[1,12], **Helen J. Lachmann**[13], **Andrew P. Cope**[14], **Katrin D. Mayer-Barber**[15], and **Claudia Kemper**[1,2,†]

[1]MRC Centre for Transplantation, Division of Transplant Immunology and Mucosal Biology, King's College London, London SE1 9RT, UK. [2]Laboratory of Molecular Immunology and Immunology Center, National Heart, Lung, and Blood Institute, Bethesda, MD 20892, USA. [3]Institute for Molecular Bioscience and School of Biomedical Sciences, University of Queensland, QLD 4072, Australia. [4]Institute for Medical Microbiology and Hospital Epidemiology, Medizinische Hochschule Hannover, 30625 Hannover, Germany. [5]Pathology Core, National Heart, Lung, and Blood Institute, Bethesda, MD 20892, USA. [6]School of Biochemistry and Immunology, Trinity College Dublin, Dublin, Ireland. [7]Laboratory of Parasitic Diseases, National Institute of Allergy and Infectious Diseases, Bethesda, MD 20892, USA. [8]Institute for Systemic Inflammation Research, University of Lübeck, Lübeck, Germany. [9]Division of Immunobiology, Cincinnati Children's Hospital Medical Center and University of Cincinnati College of Medicine, Cincinnati, OH, USA. [10]Department of Infection and Immunity, University of Sheffield, Sheffield S10 2RX, UK. [11]Genomics Centre, Faculty of Life Sciences and Medicine, King's College London, London SE1 9NH, UK. [12]Lymphocyte Cell Biology Section, Molecular Immunology and Inflammation Branch, National Institute of Arthritis and Musculoskeletal and Skin Diseases, Bethesda, MD 20892, USA. [13]UK National Amyloidosis Centre, Division of Medicine, University College London, Royal Free Campus, London NW3 2PF, UK. [14]Academic Department of Rheumatology, Division of Immunology, Infection and Inflammatory Diseases, King's College London, London SE1 1UL, UK. [15]Laboratory of Clinical Infectious Diseases, Inflammation and Innate Immunity Unit, National Institute of Allergy and Infectious Diseases, Bethesda, MD 20892, USA.

[#] These authors contributed equally to this work.

Abstract

The NLRP3 inflammasome controls interleukin-1β maturation in antigen-presenting cells, but a direct role for NLRP3 in human adaptive immune cells has not been described. We found that the

[†]Corresponding author. claudia.kemper@kcl.ac.uk.

The authors declare no competing financial interests.

SUPPLEMENTARY MATERIALS

www.sciencemag.org/content/352/6292/aad1210/suppl/DC1

Materials and Methods

Figs. S1 to S9

Tables S1 to S5

NLRP3 inflammasome assembles in human CD4+ T cells and initiates caspase-1–dependent interleukin-1β secretion, thereby promoting interferon-γ production and T helper 1 (T_H1) differentiation in an autocrine fashion. NLRP3 assembly requires intracellular C5 activation and stimulation of C5a receptor 1 (C5aR1), which is negatively regulated by surface-expressed C5aR2. Aberrant NLRP3 activity in T cells affects inflammatory responses in human autoinflammatory disease and in mouse models of inflammation and infection. Our results demonstrate that NLRP3 inflammasome activity is not confined to "innate immune cells" but is an integral component of normal adaptive T_H1 responses.

The complement system is an ancient innate immune sensor system that is essential for elimination of pathogens by the host. Processing in serum of liver-derived C3 into C3a and C3b and of C5 into C5a and C5b activation fragments leads to opsonization and removal of invading microbes, mobilization of innate immune cells, and induction of inflammatory reactions (1). However, complement also profoundly regulates adaptive immunity: In addition to T cell receptor (TCR) activation, costimulation, and the presence of interleukin (IL)–12 (2), human CD4+ T cells also depend on the activation of T cell–expressed complement receptors binding C3 activation fragments for normal T helper 1 (T_H1) induction (3). Unexpectedly, the engagement of complement receptors on T cells is independent of systemic complement but instead is mediated in an autocrine manner by complement activation fragments produced by the T cell itself. In particular, C3a and C3b are generated intracellularly via cathepsin L–mediated cleavage of C3 in T cells upon TCR activation (4). These engage their respective receptors—a G protein–coupled receptor (GPCR) C3a receptor (C3aR) and the complement regulator CD46 (which binds C3b)—and induce autocrine interferon-γ (IFN-γ) (5, 6). Mechanistically, C3aR- and CD46-mediated signals (i) regulate IL-2R assembly, (ii) up-regulate the glucose transporter GLUT1 and the amino acid transporter LAT1, and (iii) up-regulate mTORC1 activation, which is required for the metabolic programming essential for IFN-γ induction (7).

However, CD46 costimulation is not only essential for IFN-γ production and human T_H1 induction; it also contributes to the negative control of T_H1 responses. Together with IL-2, CD46-mediated signals drive the coexpression of immunosuppressive IL-10 in T_H1 cells and initiate their switch into a (self-)regulatory and contracting phase (3). Accordingly, C3- and CD46-deficient patients suffer from recurrent infections and have severely reduced T_H1 responses in vitro and in vivo, whereas T_H2 responses remain intact (5, 8). Conversely, uncontrolled intracellular C3 activation (or dysregulated CD46 engagement) in T cells contributes to hyperactive T_H1 responses observed in autoimmunity (3, 4, 9) that can be normalized pharmacologically by targeting intracellular cathepsin L function (4). Of note, CD46 is not expressed on somatic tissue in rodents and a functional homolog has not yet been identified. This indicates the existence of substantial differences in the complement receptor–driven pathways regulating T cell responses between species [reviewed in (6)].

Given the critical role of intracellular C3 processing in human T_H1 induction and contraction and the importance of C5a generation in inflammation, we investigated whether human CD4+ T cells also harbor an "intracellular C5 activation" system contributing to effector responses.

Autocrine activation of C5a receptors regulates IFN-γ production by human CD4+ T cells

Human CD4+ T lymphocytes isolated from healthy donors contained intracellular stores of C5 and produced low levels of C5a in the resting state. TCR activation, in particular TCR + CD46 costimulation, increased the amounts of intracellular C5a, and this was associated with the secretion of C5a to the cell surface (Fig. 1, A and B). C5a, as well as the C5a "des-arginized" form of C5a (C5adesArg) generated by carboxypeptidase processing, can bind two distinct GPCR receptors, C5aR1 (CD88) and C5aR2 (GPR77, C5L2) (10, 11). Binding of C5a to C5aR1 preferentially mediates proinflammatory responses. The function of C5aR2 varies with cell type; C5aR2 can act either as a nonsignaling decoy receptor antagonizing C5aR1 or as an active transducer of pro- or anti-inflammatory signals (11–14).

Both extra- and intracellular localization of C5aR1 and C5aR2 on human monocytes have been reported (14, 15), but expression patterns in human CD4+ T cells have not been described in detail. We detected expression of both *C5AR1* and *C5AR2* mRNA in human CD4+ T cells (Fig. 1C) and protein by immunoblotting (fig. S1A), confocal microscopy (Fig. 1D), and flow cytometry (Fig. 1, E and F). Although mRNA amounts for *C5aR1* and *C5aR2* vary in T cells (Fig. 1C) (16), the protein levels for these receptors are comparable among donors (Fig. 1E). In resting and activated CD4+ T cells, C5aR1 is expressed exclusively intracellularly and in low amounts, whereas the C5aR2 receptor is abundantly present inside and to a lesser degree on the cell surface (Fig. 1F). Using human embryonic kidney (HEK) 293 cells that had been stably transfected to express C5aR1, C5aR2, or no receptor, we corroborated the specificity of reagents used for C5a receptor detection (fig. S1, B and C). Competitive binding studies of C5a labeled with radioactive ^{125}I (Fig. 1G and fig. S1D) confirmed the ability of resting and activated human CD4+ T cells to bind C5a.

To determine whether autocrine engagement of the C5a receptors on T cells regulates T_H1 induction, we activated human CD4+ T cells with immobilized antibodies to CD3, CD3 and CD28, or CD3 and CD46 in the presence or absence of (i) a specific antagonist to C5aR1 [PMX53 (17)]; (ii) the C5aR1/C5aR2 receptor double antagonist A8$^{\Delta 71\text{-}73}$ [dRA (18)], targeting only C5aR2 (as the C5aR1 is expressed intracellularly); or (iii) a specific C5aR2 agonist (19). All reagents were cell-impermeable. Blocking C5aR2 activity significantly increased T_H1 induction (Fig. 1H, left), and activating C5aR2 with the agonist or with C5a or C5adesArg reduced T_H1 responses (Fig. 1H, middle, and fig. S1E). Blockade of C5aR2 also led to increased T_H17 (IL-17) but not T_H2 (IL-4) responses (fig. S1F) without altering cell viability (fig. S1G). Consistent with the solely intracellular localization of C5aR1, the C5aR1-specific antagonist had no effect on IFN-γ production because it could not "reach" and block intracellular C5aR1 (Fig. 1H, right). However, reduction of intracellular C5aR1 by small interfering RNA (siRNA) gene targeting led to a commensurate decrease in IFN-γ production (Fig. 1I and fig. S1H). Together, these data show that intracellular C5 activation contributes to induction of IFN-γ production in CD4+ T cells via intracellular C5aR1 engagement, and that the surface-expressed C5aR2 exerts negative control of IFN-γ, possibly via suppression of intracellular C5aR1 signals.

Canonical NLRP3 inflammasome activation in CD4+ T cells enhances IFN-γ production

To delineate the autocrine C5-driven pathways contributing to regulation of IFN-γ in $CD4^+$ T cells, we performed a transcriptome analysis using T cells from three healthy donors activated, or not, with anti-CD3 and anti-CD46 in the presence or absence of the C5aR1/C5aR2 antagonist. Surprisingly, we observed enrichment of transcripts associated with inflammasome activation, including *NLRP3* and *IL1B* (Fig. 2, A and B, and table S1), in cells activated with anti-CD3 and anti-CD46. Inhibition of C5aR2 during these activation conditions further increased some of these transcripts, notably *IL1A* and *IL1B* (fig. S2A and table S2); this finding offers further support for the idea that blocking C5aR2 leads to unrestrained or increased engagement of intracellular C5aR1 driven by the anti-CD3– and anti-CD46–induced increase in intracellular C5a generation.

IL-1α and IL-1β are prototypical proinflammatory cytokines involved in innate immune responses and contributing to the development of several pathogenic autoimmune diseases, including type 1 diabetes and arthritis (20–22). Both IL-1α and IL-1β bind to IL-1 receptor 1 (IL-1R1). Antigen-presenting cell (APC)–derived IL-1β supports T cell priming and imprinting of T helper effector function (23), including enhancement of IFN-γ and IL-17 production from $CD4^+$ T cells (24–26). Further, mice with deletion of the IL-1β signal transducer MyD88 in T lymphocytes cannot generate memory T cells (27). Pro–IL-1β is synthesized as a 31-kDa precursor and converted to mature 17-kDa IL-1β via caspase-1 cleavage (28). Caspase-1 is regulated by proteolytic activation during oligomerization with NLRP3 and the adaptor ASC (apoptosis-associated speck-like protein containing a caspase recruitment domain), which is triggered in response to danger signals (29, 30). NLRP3 inflammasome function requires a priming signal 1 (which induces *NLRP3* and *IL1B* gene transcription) and a signal 2 that induces functional inflammasome assembly (30) and has been described in myeloid innate immune cells, with monocytes as the main source of IL-1β (25, 31), and in several nonimmune cell types (such as microglia, endothelial cells, and retinal pigment epithelial cells) (32–34). However, canonical NLRP3 inflammasome activity has not been demonstrated in lymphoid adaptive immune cells.

We confirmed the presence of an "NLRP3 signature" in T cells by demonstrating *NLRP3* and *IL1B* gene (fig. S2B) and protein expression, as well as generation of activated caspase-1 and mature IL-1β, in activated human $CD4^+$ T cells (Fig. 2, C and D, and fig. S2, C to F). Consistent with our gene array data, anti-CD3 and anti-CD46 activation led to robust NLRP3 activation and IL-1β generation (Fig. 2D) and increased colocalization of NLRP3 and ASC (Fig. 2E). Notably, both resting naïve and memory $CD4^+$ T cells expressed NLRP3 protein (fig. S2, C and D).

Because IL-1β supports T_H1 induction (35) and is most strongly induced by the T_H1 driver CD46, we next assessed whether inhibition of NLRP3 activity in $CD4^+$ T cells perturbs IFN-γ production. To this end, $CD4^+$ T cells were activated in the presence of MCC950, a specific NLRP3 inhibitor (36), and T_H1, T_H2, and T_H17 cytokine production was measured 36 hours after activation. NLRP3 inhibition during T cell activation specifically attenuated IFN-γ (Fig. 2F), whereas differences in IL-4 and IL-17 production did not reach

significance (fig. S2G) and cell viability was unaffected (fig. S2H). The effects of the NLRP3 inhibitor could be fully reversed by the addition of recombinant human IL-1β (rhIL-1β) to cultures (Fig. 2G). Similarly, reduction of active caspase-1 activity by the specific inhibitor Z-YV AD-FMK repressed IL-1β and IFN-γ secretion (Fig. 2H and fig. S2I), and rhIL-1β provision normalized T_H1 induction in these cultures. The role for IL-1β as critical autocrine "T_H1 supporter" is reinforced by our observation that no IL-18 [which also depends on NLRP3 activation and can support T_H1 responses (37)] was measurable in our cultures and that addition of IL-18 binding protein had no effect on cytokine production (fig. S2J).

The hyperactive in vitro T_H1 response in CAPS patients is normalized by NLRP3 inhibition

To further explore this pathway, we measured the effects of NLRP3 hyperactivity in $CD4^+$ T cells isolated from the blood of patients with distinct gain-of-function mutations in NLRP3 (patient characteristics are summarized in table S3). This class of NLRP3 mutations is associated with a group of heritable monogenic syndromes known as cryopyrin-associated periodic syndromes (CAPS), characterized by excessive production of IL-1β from APCs with recurrent fevers, skin rashes, joint and ocular inflammation, and amyloidosis (38). Therapeutic suppression of the inflammatory responses can be achieved by IL-1R blockade with anakinra, an IL-1R antagonist, or canakinumab, a monoclonal antibody (mAb) targeting IL-1β (38, 39). Despite their medication regimen and the fact that cytokine production by immune cells from CAPS patients can vary with their respective "flare status" (40), T cells from a first cohort of CAPS patients that we assessed had significantly increased IL-1β secretion relativeto sex- and age-matched healthy donors (Fig. 3A), indicating that increased NLRP3 activity in $CD4^+$ T cells indeed induces heightened IL-1β secretion.

We next performed a more in-depth analysis of T cell in vitro responses from another cohort of seven CAPS patients (table S4). All patients had a naïve versus memory T cell distribution comparable to those of healthy donors (fig. S3A), and T cells from five patients of this second cohort also showed significantly increased IL-1β secretion upon activation (Fig. 3B). Furthermore, $CD4^+$ T cells from these patients trended toward substantially increased IFN-γ relative to T cells from sex- and age-matched healthy donors, and we observed a statistically significant correlation between increased IL-1β and IFN-γ secretion (Fig. 3, C and D).

T cells from CAPS patients displayed significantly reduced in vitro IL-17 responses (Fig. 3E). Although caspase-1 activity was not significantly increased in the patients' T cells at the time point assessed (36 hours), the patients with highest IL-1β secretion also had the highest active caspase-1 levels (fig. S3B). Activation of $CD4^+$ T cells from CAPS patients in the presence of the NLRP3 inhibitor MCC950 led to a reduction of both IL-1β and IFN-γ secretion (Fig. 3F). Together, these data demonstrate that human $CD4^+$ T cells produce IL-1β in an NLRP3-dependent manner, that autocrine IL-1β generation supports IFN-γ secretion, and that dysregulation of this pathway occurs in human autoinflammatory disease.

C5a receptors modulate NLRP3 inflammasome activity to regulate IFN-γ production

We next asked whether C5aR signaling could directly regulate NLRP3 activity in human CD4+ T cells. C5aR2 blockade in CD3 + CD46–activated T cells further increased *IL1B* but not *NLRP3* mRNA (fig. S4, A and B). Enhanced IFN-γ secretion driven by C5aR2 blockage could be reversed by inhibition of NLRP3 with MCC950 (Fig. 4A) without affecting IL-17 or IL-4 production (fig. S4C). Pharmacological targeting of C5aR2 via either dRA (blockage of C5aR2 signaling) or a C5aR2 agonist (activation of C5aR2 signaling) revealed that C5aR2 negatively regulates active caspase-1 and mature IL-1β expression in T cells (Fig. 4, B to D) but does not affect NLRP3 protein levels per se (fig. S4D). Silencing of *C5AR1* expression had also no effect on NLRP3 protein levels (fig. S4E) but reduced active caspase-1 (Fig. 4E) and IL-1β expression (Fig. 4F). Moreover, the reduction of IFN-γ secretion after *C5AR1* gene silencing was "rescued" by addition of rhIL-1β (Fig. 4G). Together, these data suggest that CD46-mediated signals increase *NLRP3* mRNA expression in T cells, whereas C5aR1 supports subsequent NLRP3 assembly and C5aR2 is a negative regulator of this process.

Reactive oxygen species (ROS) are "classical" upstream stimulators (signal 2) of NLRP3 assembly (41) and are strongly induced by C5aR1 in monocytes and neutrophils (42). Furthermore, generation of ROS within CD4+ T cells is required for T cell activation and induction of IL-2, a key cytokine for T_H1 biology (43). We therefore assessed whether autocrine C5aR1 engagement by intracellular C5a generation in T cells induces NLRP3 inflammasome assembly via ROS generation. We observed potent generation of ROS in anti-CD3– and anti-CD46–induced T_H1 cells (Fig. 5A) and poor T_H1 induction in the presence of a ROS inhibitor (Fig. 5B). Further, reduction of C5aR1 protein expression by gene silencing decreased ROS production (Fig. 5C, left), whereas inhibition of C5aR2 surface activation significantly increased ROS generation in T cells (Fig. 4C, right).

Enhanced IFN-γ production by T cells induced by C5aR2 blockade could be entirely reversed by the presence of a ROS inhibitor (Fig. 5B and fig. S5). This finding suggests that NLRP3 activation in human T cells involves intracellular C5-driven ROS production.

NLRP3 activity in CD4+ T cells is required for optimal IFN-γ responses during viral infection

To address the biological importance of NLRP3-driven autocrine IL-1β production by CD4+ T cells, we analyzed CD4+ T cell responses of *Nlrp3*$^{-/-}$, *Il1a*$^{-/-}$/*Il1b*$^{-/-}$, and *Il1r1*$^{-/-}$ mice initially in vitro and subsequently in an established in vivo viral infection model. Similar to human CD4+ lymphocytes, CD4+ cells from wild-type mice expressed NLRP3 and IL-1β; neither NLRP3 nor IL-1β mRNA (Fig. 6A) and protein (fig. S6A) were detectable in T cells from respective gene-deficient animals. We observed no difference in the proportion of naïve versus memory T cells or in T cell survival between wild-type and knockout strains (fig. S6, B and C). However, upon in vitro CD3 + CD28 activation, CD4+ T cells from *Nlrp3*$^{-/-}$, *Il1a*$^{-/-}$/*Il1b*$^{-/-}$, and *Il1r1*$^{-/-}$ mice had a reduction of ~75% in IFN-γ production when

compared to T cells from wild-type animals (Fig. 6B); in contrast, IL-10, IL-4, and IL-17 production were unaffected in all three mouse mutant lines (fig. S6D). Further, although activation of T cells from wild-type mice in the presence of the NLRP3 inhibitor MCC950 had no effect on cell viability (fig. S6E), only IFN-γ production was significantly reduced (Fig. 6C and fig. S6F). These results indicate that diminished IFN-γ secretion in the "knockout T cells" was not due to a developmental defect, whereas NLRP3 activity is required for normal IFN-γ induction. Moreover, both naïve and memory mouse $CD4^+$ T cells displayed a requirement for NLRP3-driven IL-1β activity for optimal IFN-γ secretion (fig. S6, G and H).

Using a lymphocytic choriomeningitis virus (LCMV) model (Fig. 6D), we next demonstrated an in vivo role for NLRP3-driven IL-1β generation in T_H1 responses during infection. Irradiated mice were reconstituted with equal parts bone marrow cells isolated from wild-type mice mixed with bone marrow cells from *Nlrp3*$^{-/-}$, *Il1a*$^{-/-}$/*Il1b*$^{-/-}$, or *Il1r1*$^{-/-}$ mice before infection with LCMV. Analysis of splenic $CD4^+$ T cells 12 days after infection revealed comparable numbers of GP66-77$^+$Ki67$^+$ LCMV tetramer$^+$ cells generated by all animals (Fig. 6, E and F), indicating that *Nlrp3*$^{-/-}$, *Il1a*$^{-/-}$/*Il1b*$^{-/-}$, and *Il1r1*$^{-/-}$ $CD4^+$ T cells survived normally. However, T cells deficient in any of these components displayed substantially reduced ability to generate IFN-γ$^+$ virus-specific cells in vivo (with an average decrease of ~50%) (Fig. 6, G and H). Together, these data demonstrate that autocrine canonical NLRP3 inflammasome activity is required for optimal protective IFN-γ production by $CD4^+$ T cells during viral infection.

Autocrine NLRP3 activity in T cells controls the T_H1-T_H17 balance during intestinal inflammation

To further substantiate the in vivo importance of NLRP3 inflammasome activity in $CD4^+$ T cells, we also measured the effects of NLRP3 deficiency in an autoimmune disease setting by assessing its influence on disease outcome in a $CD4^+$ T cell transfer model of colitis, where IL-1β and both T_H1 and T_H17 responses in the intestine have been shown to be involved (44, 45). To this end, sorted $CD4^+CD25^-CD45RB^{hi}$ T cells isolated from C57BL/6 wild-type or *Nlrp3*$^{-/-}$ mice were injected intraperitoneally (i.p.) into age- and sex-matched C57BL/10 *Rag2*$^{-/-}$ mice. Body weight and disease score were monitored and cytokine production by lamina propria $CD4^+$ T cells measured after animals displayed disease symptoms and were killed. Unexpectedly, relative to mice injected with wild-type $CD4^+$ T cells, mice that had received *Nlrp3*$^{-/-}$ $CD4^+$ T cells developed more severe disease with significantly increased weight loss, reduction in colon length, and higher disease scores (Fig. 7, A to C). Similar to our observation in the LCMV model, colonic *Nlrp3*$^{-/-}$ T cells displayed a substantial reduction in IFN-γ production (average decrease ~45%); however, we also observed a concurrent significant increase in T_H17 responses in these animals (Fig. 7, D and E). These observations were confirmed using a $CD4^+$ T cell–driven model of graft-versus-host disease (GvHD) where mice receiving *Nlrp3*$^{-/-}$ T cells also displayed more severe illness with reduced T_H1 but concurrently increased T_H17 induction (fig. S7, A to D). Together, these data demonstrate that the NLRP3 inflammasome mediates functionally important $CD4^+$ T cell intrinsic effects that not only are required for normal IFN-γ

production but also control the T_H1-T_H17 balance during (at minimum) intestinal inflammation. These latter findings align with our observation that T cells from CAPS patients indeed have increased T_H1 but also decreased in vitro T_H17 responses (Fig. 3, C and E).

Discussion

Our results show that canonical NLRP3 inflammasome function is not confined to innate immune cells but is operative in adaptive $CD4^+$ T cells and, via autocrine IL-1β activity, is required for the optimal production of the key host defense factor IFN-γ. Further, and unexpectedly, NLRP3 assembly in human T cells requires TCR-induced intracellular C5 activation and stimulation of intracellular C5aR1, which initiates the generation of ROS and thereby provides a critical signal 2 for inflammasome assembly (30). Secretion of intracellularly generated C5a/C5ades-Arg engages the surface-expressed "alternative" C5aR2, which negatively controls NLRP3 activation either through inhibition of the C5aR1 or via a yet undefined mechanism. Given that APCs provide generally ample amounts of IL-1β during the cognate APC/T cell interaction, our observation that normal IFN-γ production requires also T cell autocrine IL-1β production is initially somewhat surprising. However, we envisage that, whereas APC-derived NLRP3-activated IL-1β supports initial T_H1 priming, proper "imprinting" or maintenance of the T_H1 phenotype during differentiation and migration into the periphery may rely on autocrine NLRP3 activity. IL-1β production by T cells, relative to myeloid cells, is comparatively low and, as we have shown, tightly regulated by an autocrine C5aR1 versus C5aR2 activation balance. The likely reason for this is that rapid control of local IL-1β is critical to normal termination of T_H1 responses: Human T_H1 cells co-induce IL-10 secretion in a CD46-dependent fashion during their contraction phase, and failure of this "IL-10 switch" underlies hyperactive T_H1 responses observed in rheumatoid arthritis and multiple sclerosis (3, 9). IL-1β is a strong suppressor of IL-10 production (23) and, accordingly, we found that blockade of C5aR2 increased the IFN-γ/IL-10 ratio in $CD4^+$ T cells (fig. S8A), whereas IL-1β addition to cultures increased IFN-γ (Fig. 2G) but blocked proportional IL-10 secretion (fig. S8B). Moreover, IFN-γ to IL-10 switching was significantly reduced in T cells from CAPS patients (fig. S8C).

Further supporting the notion that autocrine T cell cytokine production needs to be carefully controlled in the microenvironment is our observation that the reduction in IFN-γ secretion by T cells from *Nlrp3*$^{-/-}$ mice led to a concurrent increase in colonic lamina propria T_H17 cells and increased intestinal inflammation. These findings demonstrate that T_H1 cells negatively control the influx and/or expansion of T_H17 cells during colitis and that T_H17 induction at this location (and in this model) is independent of intrinsic T cell NLRP3 activity. These observations may also help to explain why some groups observed protection of *Nlrp3*$^{-/-}$ animals in models of inflammatory bowel disease while others observed aggravated disease (46, 47); these earlier studies had not controlled for a T cell–intrinsic function of the NLRP3 inflammasome. Also, because IL-1β also boosts the production of other cytokines including IL-4 and IL-17 (35), the activation of the NLRP3 inflammasome in T cells and its functional outcome could be context-dependent. For example, Bruchard *et al.* recently observed a noncanonical function for NLRP3 in mouse $CD4^+$ T cells (they did

not assesses human T cells) independent of inflammasome formation and IL-1β secretion, during T_H2 induction and tumor growth (48).

In addition, there are clear species-specific differences in the relative contributions of complement receptor activities to IL-1β and/or IFN-γ induction in $CD4^+$ T cells. Although we found that $CD4^+$ T cells from *C5ar2*$^{-/-}$ mice have increased in vitro IFN-γ production, which was reduced to normal levels by MCC950 treatment (fig. S9), and *C5ar1*$^{-/-}$ mice have impaired in vitro and in vivo T_H1 responses (49), the role and expression of anaphylatoxin receptors on mouse T cells remains a matter of controversy (49–51). But more important, mice lack expression of CD46 on all immune cells (6), whereas in humans, CD46 costimulation is required for IL-2R assembly and the metabolic reprogramming in $CD4^+$ T cells that drives IFN-γ secretion (5, 7, 52). Further, we show here that CD46 engagement, aside from amplifying intracellular C5a generation and ROS production (signal 2), also delivers an important signal 1 for NLRP3 inflammasome activation by mediating increased transcription of the *NLRP3* gene [this likely occurs via CD46-induced increased NF-κB nuclear translocation during T cell activation (6)]. Because a functional homolog for CD46 has not been identified in rodents, the exact upstream signals controlling NLRP3 inflammasome activation and IL-1β production in murine T cells remain to be defined.

In summary, the regulated cross-talk between intracellularly activated complement components (“complosome”) and the NLRP3 inflammasome emerges as fundamental to human T_H1 induction and regulation. That established innate immune pathways previously not thought to be operative in adaptive immune cells are not only present but also are key in directing immunological responses is of substantial importance to our understanding of immunobiology and immune system evolution. Further, the possibility that this normal functional cross-talk may also be target of viral immune evasion strategies (53) suggests that the complement-NLRP3 axis in T cells could represent a novel therapeutic target for the modulation of IFN-γ responses in autoimmunity and infection. In this regard, it will be valuable to explore whether optimal production of IFN-γ by $CD8^+$ T cells (54), natural killer T (NKT) cells, and/or innate lymphoid type 1 (ILC1) cells also relies on autocrine complement-NLRP3 inflammasome activity.

Materials and methods

Healthy donors and patients

Blood samples were obtained with ethical and institutional approvals (Wandsworth Research Ethics Committee, REC number 09/H0803/154). T cells were purified blood samples from healthy volunteers after informed consent. Fourteen adult patients with CAPS were recruited at the National Amyloidosis Centre, University College London (ethical approval REC reference number 06/Q0501/42) with key information on the patients summarized in tables S3 and S4. In all experiments that involved T cells from CAPS patients, T cells from age- and sex-matched healthy volunteers were used as controls.

Mice used in the study

All mice used in this study are on a C57BL/6 background (with the exception of the GvHD experiment, where Balb/c mice were used). Wild-type and *Il1r1*$^{-/-}$ mice were purchased from Jackson Laboratories and subsequently backcrossed to B6 for 10 generations at NIH (Bar Harbor, ME). The *C5ar2*$^{-/-}$ (human gene symbol GPR77) mice were previously described (12), *Nlrp3*$^{-/-}$ animals were provided by V. Dixit of Genentech, and mice deficient in *Il1a* and *Il1b* (*Il1a/Il1b*$^{-/-}$ animals) were kindly provided by Y. Iwakura (Tokyo University) (55). The C57BL/10 RAG2$^{-/-}$ mice were obtained from Taconic. All animals were maintained in AALAC-accredited BSL2 or BSL3 facilities at the NIH or FDA and experiments performed in compliance with an animal study proposal approved by the NIAID or FDA Animal Care and Use Committee.

Cell isolation and activation

Human cells—CD4$^+$ T cells and monocytes were isolated from blood as previously published using the MACS Human CD4$^+$ Positive T cell Isolation Kit or the MACS Human CD14$^+$ Cell Positive Isolation Kit (both Miltenyi Biotech, Bisley, UK), respectively (7). Purity of bead-isolated T lymphocyte fractions was typically >98% and for monocytes >95%. For naïve and memory CD4$^+$ T cell sorting, cells were stained with appropriate antibodies (naïve cells, CD4$^+$, CD45RA$^+$, CD45RO$^-$, and CD25$^-$; memory cells, CD4$^+$, CD45RA$^-$, CD45RO$^+$, and CD25$^-$) and sorted with a BD FACSAria II Cell Sorter (KCL Flow Core facility). CD4$^+$ T cells were activated in 48-well culture plates (2.5×10^5 to 3.0×10^5 cells per well) coated with mAbs to CD3, CD28, or CD46 (2.0 μg/ml PBS each) and addition of rhIL-2 (25 U/ml), thus, under nonskewing conditions. Monocytes were activated in 24-well plates (2.5×10^5 to 5.0×10^5 cells per well) by addition of LPS (50 ng/ml). Cell viability was monitored by either propidium iodide (BD Biosciences) or the LIVE/DEAD Cell Viability Assay (Life Technologies).

Mouse cells—Single cell suspensions of spleen cells were generated and red blood cells lysed using ACK lysis buffer (Life Technologies). CD4$^+$ T cells were isolated by negative selection using the Stem Cell Technologies EasySep Mouse CD4$^+$ T Cell Isolation Kit (Tukwila, WA). To obtain pure CD4$^+$ T cell populations, CD4$^+$ cells were sorted using a FACS Aria (BD Biosciences) based on CD4$^+$ CD45.2$^+$ staining and to separate naïve versus memory CD4$^+$ T lymphocytes. T cells were sort-separated based on CD4$^+$ CD44$^+$ (memory) and CD4$^+$ CD44$^-$ (naïve) stainings. For in vitro T cell activation, 48- or 96-well plates were coated with anti-CD3 (2 μg/ml) overnight at 4°C, and CD4$^+$ T cells (0.5×10^6 to 1.0×10^6 per well of 48-well plates or 0.2×10^6 per well of 96-well plates) were added to the appropriate wells. Anti-CD28 (1 μg/ml) was added to the media to provide costimulation.

Lymphocytic choriomeningitis virus (LCMV) infection in mice

Preparation of mixed bone marrow (BM) chimeric mice—B6.SJL (CD45.1,1) mice were lethally irradiated (950 rad) and reconstituted with a total of 10^7 donor BM cells from C57BL/6 CD45.1,2 wild-type mice mixed at equal parts with BM cells from CD45.2,2 mice deficient (KO) in *Nlrp3*$^{-/-}$, *Il1r1*$^{-/-}$, or *Il1a/Il1b*$^{-/-}$. Mice were allowed to reconstitute for 10 weeks before infection with LCMV.

LCMV infection and assessment of antigen-specific CD4+ T cell response— Ten weeks after reconstitution, the mice were infected i.p. with 10^5 pfu of LCMV-Armstrong. On day 12 after infection, the mice were killed and the spleens removed for processing. For ex vivo cytokine staining of mouse cells after LCMV infection, cells were incubated with LCMV GP61-80 peptide (1 μg/ml) in the presence of monensin and brefeldin for 5 hours at 37°C. Staining for LCMV-specific $CD4^+$ T cells was performed using an APC-labeled $1A^b$ LCMV GP66-77 tetramer (NIH tetramer core facility) as described (56). Data were acquired with a FACS Calibur, Fortessa LSRIII, or FACS Aria cytometer (BD Biosciences) and analyzed with FlowJo 10.0.8 software (Ashland, OR).

Induction of colitis and colon cell isolation

Splenic $CD4^+$ T cells were isolated from C57BL/6 or *Nlpr3*$^{-/-}$ mice using a negative selection CD4 T cell enrichment kit (Stemcell tech), were stained with anti-CD45RB FITC, anti-CD25 APC, and anti-CD4 BV421, and sorted on a FACS Aria (BD biosciences) for $CD4^+$ $CD25^-CD45RB^{hi}$ (brightest 35%) cells. Wild-type or *Nlpr3*$^{-/-}$ cells (2×10^5 each) were injected i.p. into age- and sex-matched C57BL/10 $RAG2^{-/-}$ mice. The mice were killed when symptoms of clinical disease (5 to 10% weight loss of original body weight and/or diarrhea) were observed in at least one group, approximately 6 to 11 weeks after adoptive transfer. Colon lamina propria cells were isolated as described (57), with the additional step of further purifying the cells over a 44 and 67% Percoll gradient to enrich for the mononuclear cells.

Scoring of intestinal inflammation

Samples of the proximal, mid-, and distal colon were excised after feces were flushed from the colons, placed into 3.7% formaldehyde solution, and then paraffin-embedded. Cross-sectional sections were cut and stained with hematoxylin and eosin (H&E). Colon pathology scores were based on severity of mononuclear cell inflammation, intestinal wall thickening, including infiltration to the muscularis, and epithelial damage, including edema, degeneration, and necrosis on a graded scale where 0 = normal, 0.5 = very mild, 1 = mild, 2 = moderate, 3 = severe. Samples were scored blinded by a pathologist from the NIH Pathology Score.

Induction of graft versus host disease (GvHD)

Balb/c mice were lethally irradiated with 900 cGy (two doses of 450 cGy 3 hours apart) on day −1. C57BL/6 wild-type bone marrow was depleted of T cells with the use of a CD90.2 Positive Selection Kit (Stemcell tech), and 5×10^6 cells were transferred on the following day (day 0) alone (control), or in addition to 1×10^6 wild-type B6 or *Nlpr3*$^{-/-}$ naïve $CD4^+$ T cells isolated with the Negative Selection Naïve CD4 T Cell Kit (Stemcell tech). Mice were killed upon clinical symptoms of disease (diarrhea and weight loss) on day 12 after cell transfer.

Detection of active caspase-1 and reactive oxygen species (ROS)

Generation of cleaved and active caspase-1 in cells was monitored by Western blotting for appropriate active fragment generation and by using the Green FLICA Caspase-1 Assay Kit

(Immuno-Chemistry Technologies, Bloomington, MN) according to the manufacturer's protocol with subsequent FACS analysis. ROS staining was performed by incubating cells to be assayed in dihydrorhodamine 123 (17 μg/ml) diluted in Hank's balanced salt solution with 10 mM HEPES (all from Sigma Aldrich) for 15 min at 37°C. Data were acquired on a FACS Calibur or Fortessa LSRIII cytometer (BD Biosciences) and analyzed with FlowJo software.

Confocal microscopy

Cells were fixed and permeabilized using the Cytofix/Cytoperm Kit (BD Biosciences) and stained with the indicated primary antibodies overnight and with secondary antibodies for 30 min at 4°C. Cells were mounted using VECTASHIELD media with DAPI (Vector Laboratories, Burlingame, CA) and images were acquired with a Nikon A1R confocal microscope (Nikon Imaging Centre, King's College London) and analyzed using NIS Elements (Nikon) and ImageJ software (National Institutes of Health).

Binding studies with recombinant human ^{125}I-labeled C5a

$CD4^+$ T cells from healthy donors were left non-activated or activated for 4 hours with immobilized antibodies to CD3 and CD46 and then incubated for 2 hours at 4°C (1×10^7 cells/ml) with 10 μl of 0.1 nM ^{125}I-rhC5a (Perkin Elmer) and either 400 nM nonlabeled rhC5a in HAG-CM buffer (1 mM $CaCl_2$, 1 mM $MgCl_2$, 0.25% bovine serum albumin, 0.5 mM glucose, pH 7.4) or buffer without rhC5a addition. Cells were vacuum-transferred onto 96-well MultiScreen-HV filter plates (MAHVN4510; Millipore/Merck), nonbound ^{125}I-rhC5a removed by washing and cell-bound ^{125}I-rhC5a detected on the filter membranes by ^{125}I using a Packard Cobra II Gamma Counter (Perkin Elmer). For binding controls, HEK 293 cells (ATCC CRL 1573) were stably transfected with the pQCXIN vector expressing hC5aR1 or hC5aR2 (leading to expression of >1 Mio. of the respective C5aR/cell) or with the "empty" vector as control (58) (these cell lines also served as specificity controls for the anti-C5a receptor antibodies used in this study). In order to get comparable low CPM values as observed with purified T cells, only 5×10^4 cells/ml of C5aR1- or C5aR2-expressing HEK cells were applied. They were diluted in buffer containing "no-C5aR-expressing control" cells. The constant higher number of cells (5×10^5 HEK cells/ml in the 30-μl volume later used in the binding assay) permitted repetitive washing without cell loss and ensured identical nonspecific binding in all samples containing the same cell type. C5aR1-, C5aR2-expressing or control HEK 293 cells were incubated for 1 hour with or without 100 nM of nonlabeled rhC5a, washed thoroughly and then incubated for an additional 2 hours with 10 μl of 0.1 nM ^{125}I-rhC5a. After removal of nonbound rhC5a, binding of ^{125}I-C5a to the respective HEK 293 cell lines was determined by measuring gamma radioactivity. To exclude C5a-induced C5aR-internalization during all binding studies all steps in the binding experiments were performed at 4°C and HEK 293 cells were additionally preincubated 15 min at 37°C with 0.1% NaAcid and Cytochalasin B (21 μg/ml) and then cooled on ice for 5 min before their incubation with rhC5a.

Cytokine measurements

Cytokine production by cells in culture was quantified from cell supernatants using either the human or mouse $T_H1/T_H2/T_H17$ Cytometric Bead Array (BD Bioscience) or via intracellular cytokine staining after treated for 4 hours with PMA (50 ng/ml), ionomycin (1

μg/ml) (both Sigma Aldrich), and 1× Golgi Plug (BD Biosciences). Secreted human IL-1β and IL-18 were measured using the Human IL-1β/IL-1F2 DuoSet Kit or the Human IL-18 Platinum ELISA kit (R&D Systems and eBiosciences, respectively) in combination with SIGMAFAST OPD tablets (Sigma Aldrich) as substrate for detection.

RNA extraction, reverse transcription polymerase chain reaction (RT-PCR), and quantitative RT-PCR

RNA was extracted with the RNeasy Mini Kit including DNase digestion and DNA cleanup (Qiagen), and reverse transcription was performed with the One Step RT-PCR (Qiagen). For quantitative PCR, RNA was reverse-transcribed with 2.5 μM random hexamers, 1 mM dNTPs, 40 U of RiboLock RNase inhibitor, and 400 U of RevertAid H Minus Reverse Transcriptase (Thermo Scientific). Quantitative PCR was performed using KI-Q Hot Start Sybr Green Mix (Sigma Aldrich), with 150 pmol of forward and reverse primers and data acquired on the CFX96 Touch Real-Time PCR Detection System (Bio-Rad). Primer sequences are listed in table S5.

RNA silencing

SiRNA targeting human C5AR1 mRNA and control scrambled siRNA were purchased from Origene (Rockville, MD) and delivered at a final concentration of 15 nM (mixture of three different C5aR1 siRNA used at 5 nM each or scramble control at 15 nM) into primary human $CD4^+$ T cells by transfection with Lipofectamine RNAiMAX (Life Technologies) following the manufacturer's instructions. *C5AR1* mRNA level reduction was consistently about 30%.

Microarray data generation and analysis

Transcriptome profiling was performed by the KCL Genomic Centre (London) using human exon 1.0 ST arrays (Affymetrix) on $CD4^+$ T cells isolated from three different healthy donors that were left either nonactivated or were activated with antibodies to CD3 and CD46 for 2 hours in the absence or presence of the C5aR1/C5aR2 antagonist. Expression data were analyzed using Partek Genomics Suite (Partek Inc., St. Louis, MO) version 6.6 and Gene Set Enrichment Analysis, GSEA (59) (Broad Institute of MIT and Harvard) with a normalized enrichment score of 1.8 to derive normalized enrichment score (NES), nominal *P* value, and FDR *q* value. Microarray data sets were used in conjunction with the Qiagen-generated inflammasome gene set (84 members). Heat maps for the leading edge subset were drawn with Partek genomics suite. Table S1 shows the normalized read values from microarrays for Fig. 2, A and B. The list of annotated genes differentially regulated by the C5aR1/C5aR2 double antagonist (fig. S2) is given in table S2.

Statistical analysis

Analyses were performed with GraphPad Prism (La Jolla, CA). Data are presented as mean ± SEM and compared using either paired *t* tests with Bonferroni correction for multiple comparisons, one- or two-way analysis of variance (ANOVA) with a Tukey multiple comparison post hoc test or with Sidak multiple-comparisons test, as appropriate.

Correlation analysis (Fig. 3D and fig. S3B) was performed with Spearman's correlation test. *P* values < 0.05 denote statistical significance.

Supplementary Material

Refer to Web version on PubMed Central for supplementary material.

ACKNOWLEDGMENTS

We thank the healthy volunteers and the patients for their support, A. Fara and J. Sumner (King's College London) for initial contributions to the C5aR2 antagonism studies, and Y. Iwakura (Tokyo University) for providing the combined *Il1a/Il1b*$^{-/-}$ mice. The MHC class II tetramer to LCMV (GP66-77) was kindly provided by the NIH Tetramer Core. We thank the Nikon Imaging Centre and the Genomics Centre at King's College London. The data presented in this manuscript are tabulated in the main paper and in the supplementary materials. The detailed gene array data have been deposited in the GEO database with accession number GSE69090. Supported by MRC Centre grant MR/J006742/1, an EU-funded Innovative Medicines Initiative BTCURE (C.K. and A.P.C.); a Wellcome Trust Investigator Award (C.K.); a Wellcome Trust Intermediate Clinical Fellowship award (B.A.); British Heart Foundation grant PG/09/018/25279 (P.M.); Science Foundation Ireland grant G20598 and Australia National Health and Medical Research Council project grant APP1086786 (R.C.C.); the King's Bioscience Institute at King's College London (G.A.); the National Institute for Health Research (NIHR) Biomedical Research Centre based at Guy's and St. Thomas' NHS Foundation Trust and King's College London; and the Division of Intramural Research, National Heart, Lung, and Blood Institute, and the intramural research program of NIAID. T.M.W., P.M., and M.A.C. are co-inventors on a U.S. provisional patent application (62/242632) related to the C5aR2 agonist used this manuscript. J.K. is inventor on U.S. patent 8/542,862, which was filed by Cincinnati Children's Hospital related to the C5aR1/C5aR2 antagonist A8D71-73.

REFERENCES

1. Ricklin D, Hajishengallis G, Yang K, Lambris JD. Complement: A key system for immune surveillance and homeostasis. Nat. Immunol. 2010; 11:785–797. doi: 10.1038/ni.1923; pmid: 20720586. [PubMed: 20720586]
2. Murphy KM, Stockinger B. Effector T cell plasticity: Flexibility in the face of changing circumstances. Nat. Immunol. 2010; 11:674–680. doi: 10.1038/ni.1899; pmid: 20644573. [PubMed: 20644573]
3. Cardone J, et al. Complement regulator CD46 temporally regulates cytokine production by conventional and unconventional T cells. Nat. Immunol. 2010; 11:862–871. doi: 10.1038/ni.1917; pmid: 20694009. [PubMed: 20694009]
4. Liszewski MK, et al. Intracellular complement activation sustains T cell homeostasis and mediates effector differentiation. Immunity. 2013; 39:1143–1157. doi: 10.1038/ni.1917; pmid: 20694009. [PubMed: 24315997]
5. Le Friec G, et al. The CD46-Jagged1 interaction is critical for human TH1 immunity. Nat. Immunol. 2012; 13:1213–1221. doi: 10.1038/ni.2454; pmid: 23086448. [PubMed: 23086448]
6. Yamamoto H, Fara AF, Dasgupta P, Kemper C. CD46: The 'multitasker' of complement proteins. Int. J. Biochem. Cell Biol. 2013; 45:2808–2820. doi: 10.1016/j.biocel.2013.09.016; pmid: 24120647. [PubMed: 24120647]
7. Kolev M, et al. Complement regulates nutrient influx and metabolic reprogramming during Th1 cell responses. Immunity. 2015; 42:1033–1047. doi: 10.1016/j.immuni.2015.05.024; pmid: 26084023. [PubMed: 26084023]
8. Ghannam A, et al. Human C3 deficiency associated with impairments in dendritic cell differentiation, memory B cells, and regulatory T cells. J. Immunol. 2008; 181:5158–5166. doi: 10.4049/jimmunol.181.7.5158; pmid: 18802120. [PubMed: 18802120]
9. Astier AL, Meiffren G, Freeman S, Hafler DA. Alterations in CD46-mediated Tr1 regulatory T cells in patients with multiple sclerosis. J. Clin. Invest. 2006; 116:3252–3257. doi: 10.1172/JCI29251; pmid: 17099776. [PubMed: 17099776]
10. Sarma JV, Ward PA. New developments in C5a receptor signaling. Cell Health Cytoskelet. 2012; 4:73–82. pmid: 23576881. [PubMed: 23576881]

11. Scola AM, Johswich KO, Morgan BP, Klos A, Monk PN. The human complement fragment receptor, C5L2, is a recycling decoy receptor. Mol. Immunol. 2009; 46:1149–1162. doi: 10.1016/j.molimm.2008.11.001; pmid: 19100624. [PubMed: 19100624]
12. Gerard NP, et al. An anti-inflammatory function for the complement anaphylatoxin C5a-binding protein, C5L2. J. Biol. Chem. 2005; 280:39677–39680. doi: 10.1074/jbc.C500287200; pmid: 16204243. [PubMed: 16204243]
13. Bamberg CE, et al. The C5a receptor (C5aR) C5L2 is a modulator of C5aR-mediated signal transduction. J. Biol. Chem. 2010; 285:7633–7644. doi: 10.1074/jbc.M109.092106; pmid: 20044484. [PubMed: 20044484]
14. Li R, Coulthard LG, Wu MC, Taylor SM, Woodruff TM. C5L2: A controversial receptor of complement anaphylatoxin, C5a. FASEB J. 2013; 27:855–864. doi: 10.1096/fj.12-220509; pmid: 23239822. [PubMed: 23239822]
15. Croker DE, Halai R, Fairlie DP, Cooper MA. C5a, but not C5a-des Arg, induces upregulation of heteromer formation between complement C5a receptors C5aR and C5L2. Immunol. Cell Biol. 2013; 91:625–633. doi: 10.1038/icb.2013.48; pmid: 24060963. [PubMed: 24060963]
16. Vogel C, Marcotte EM. Insights into the regulation of protein abundance from proteomic and transcriptomic analyses. Nat. Rev. Genet. 2012; 13:227–232. pmid: 22411467. [PubMed: 22411467]
17. Woodruff TM, et al. Therapeutic activity of C5a receptor antagonists in a rat model of neurodegeneration. FASEB J. 2006; 20:1407–1417. doi: 10.1096/fj.05-5814com; pmid: 16816116. [PubMed: 16816116]
18. Otto M, et al. C5a mutants are potent antagonists of the C5a receptor (CD88) and of C5L2: Position 69 is the locus that determines agonism or antagonism. J. Biol. Chem. 2004; 279:142–151. doi: 10.1074/jbc.M310078200; pmid: 14570896. [PubMed: 14570896]
19. Monk PN, et al. De novo protein design of agonists and antagonists of C5a receptors. Immunobiology. 2012; 217:1162–1163. doi: 10.1016/j.imbio.2012.08.097.
20. Kastbom A, et al. Genetic variation in proteins of the cryopyrin inflammasome influences susceptibility and severity of rheumatoid arthritis (the Swedish TIRA project). Rheumatology. 2008; 47:415–417. doi: 10.1093/rheumatology/kem372; pmid: 18263599. [PubMed: 18263599]
21. Pontillo A, et al. Two SNPs in NLRP3 gene are involved in the predisposition to type-1 diabetes and celiac disease in a pediatric population from northeast Brazil. Autoimmunity. 2010; 43:583–589. doi: 10.3109/08916930903540432; pmid: 20370570. [PubMed: 20370570]
22. Shaw PJ, McDermott MF, Kanneganti TD. Inflammasomes and autoimmunity. Trends Mol. Med. 2011; 17:57–64. doi: 10.1016/j.molmed.2010.11.001; pmid: 21163704. [PubMed: 21163704]
23. Zielinski CE, et al. Pathogen-induced human TH17 cells produce IFN-γ or IL-10 and are regulated by IL-1β. Nature. 2012; 484:514–518. doi: 10.1038/nature10957; pmid: 22466287. [PubMed: 22466287]
24. Sutton C, Brereton C, Keogh B, Mills KH, Lavelle EC. A crucial role for interleukin (IL)-1 in the induction of IL-17-producing T cells that mediate autoimmune encephalomyelitis. J. Exp. Med. 2006; 203:1685–1691. doi: 10.1084/jem.20060285; pmid: 16818675. [PubMed: 16818675]
25. Rao DA, Tracey KJ, Pober JS. IL-1a and IL-1b are endogenous mediators linking cell injury to the adaptive alloimmune response. J. Immunol. 2007; 179:6536–6546. doi: 10.4049/jimmunol.179.10.6536; pmid: 17982042. [PubMed: 17982042]
26. Sutton CE, et al. Interleukin-1 and IL-23 induce innate IL-17 production from γδ T cells, amplifying Th17 responses and autoimmunity. Immunity. 2009; 31:331–341. doi: 10.1016/j.immuni.2009.08.001; pmid: 19682929. [PubMed: 19682929]
27. Schenten D, et al. Signaling through the adaptor molecule MyD88 in $CD4^+$ T cells is required to overcome suppression by regulatory T cells. Immunity. 2014; 40:78–90. doi: 10.1016/j.immuni.2013.10.023; pmid: 24439266. [PubMed: 24439266]
28. Arend WP, Palmer G, Gabay C. IL-1, IL-18, and IL-33 families of cytokines. Immunol. Rev. 2008; 223:20–38. doi: 10.1111/j.1600-065X.2008.00624.x; pmid: 18613828. [PubMed: 18613828]
29. Martinon F, Tschopp J. NLRs join TLRs as innate sensors of pathogens. Trends Immunol. 2005; 26:447–454. doi: 10.1016/j.it.2005.06.004; pmid: 15967716. [PubMed: 15967716]

30. Dowling JK, O'Neill LA. Biochemical regulation of the inflammasome. Crit. Rev. Biochem. Mol. Biol. 2012; 47:424–443. doi: 10.3109/10409238.2012.694844; pmid: 22681257. [PubMed: 22681257]

31. Dinarello CA. Biologic basis for interleukin-1 in disease. Blood. 1996; 87:2095–2147. doi: 10.1111/j.1600-065X.2008.00624.x; pmid: 18613828. [PubMed: 8630372]

32. Heneka MT, et al. NLRP3 is activated in Alzheimer's disease and contributes to pathology in APP/PS1 mice. Nature. 2013; 493:674–678. doi: 10.1038/nature11729; pmid: 23254930. [PubMed: 23254930]

33. Shahzad K, et al. Nlrp3-inflammasome activation in nonmyeloid-derived cells aggravates diabetic nephropathy. Kidney Int. 2015; 87:74–84. doi: 10.1038/ki.2014.271; pmid: 25075770. [PubMed: 25075770]

34. Tseng WA, et al. NLRP3 inflammasome activation in retinal pigment epithelial cells by lysosomal destabilization: Implications for age-related macular degeneration. Invest. Ophthalmol. Vis. Sci. 2013; 54:110–120. doi: 10.1167/iovs.12-10655; pmid: 23221073. [PubMed: 23221073]

35. Ben-Sasson SZ, et al. IL-1 acts directly on CD4 T cells to enhance their antigen-driven expansion and differentiation. Proc. Natl. Acad. Sci. U.S.A. 2009; 106:7119–7124. doi: 10.1073/pnas.0902745106; pmid: 25686105. [PubMed: 19359475]

36. Coll RC, et al. A small-molecule inhibitor of the NLRP3 inflammasome for the treatment of inflammatory diseases. Nat. Med. 2015; 21:248–255. pmid: 25686105. [PubMed: 25686105]

37. Okamura H, et al. Cloning of a new cytokine that induces IFN-γ production by T cells. Nature. 1995; 378:88–91. doi: 10.1038/378088a0; pmid: 7477296. [PubMed: 7477296]

38. Menu P, Vince JE. The NLRP3 inflammasome in health and disease: The good, the bad and the ugly. Clin. Exp. Immunol. 2011; 166:1–15. doi: 10.1038/378088a0; pmid: 7477296. [PubMed: 21762124]

39. Lachmann HJ, et al. In vivo regulation of interleukin 1β in patients with cryopyrin-associated periodic syndromes. J. Exp. Med. 2009; 206:1029–1036. doi: 10.1084/jem.20082481; pmid: 19364880. [PubMed: 19364880]

40. Carta S, et al. Cell stress increases ATP release in NLRP3 inflammasome-mediated autoinflammatory diseases, resulting in cytokine imbalance. Proc. Natl. Acad. Sci. U.S.A. 2015; 112:2835–2840. doi: 10.1073/pnas.1424741112; pmid: 25730877. [PubMed: 25730877]

41. Schroder K, Zhou R, Tschopp J. The NLRP3 inflammasome: A sensor for metabolic danger? Science. 2010; 327:296–300. doi: 10.1126/science.1184003; pmid: 20075245. [PubMed: 20075245]

42. Samstad O, et al. Cholesterol crystals induce complement-dependent inflammasome activation and cytokine release. J. Immunol. 2014; 192:2837–2845. doi: 10.1126/science.1184003; pmid: 20075245. [PubMed: 24554772]

43. Sena LA, et al. Mitochondria are required for antigen-specific T cell activation through reactive oxygen species signaling. Immunity. 2013; 38:225–236. doi: 10.1016/j.immuni.2012.10.020; pmid: 23415911. [PubMed: 23415911]

44. Coccia M, et al. IL-1β mediates chronic intestinal inflammation by promoting the accumulation of IL-17A secreting innate lymphoid cells and $CD4^+$ Th17 cells. J. Exp. Med. 2012; 209:1595–1609. doi: 10.1084/jem.20111453; pmid: 22891275. [PubMed: 22891275]

45. Neurath MF. Cytokines in inflammatory bowel disease. Nat. Rev. Immunol. 2014; 14:329–342. doi: 10.1038/nri3661; pmid: 24751956. [PubMed: 24751956]

46. Bauer C, Duewell P, Lehr HA, Endres S, Schnurr M. Protective and aggravating effects of Nlrp3 inflammasome activation in IBD models: Influence of genetic and environmental factors. Dig. Dis. 2012; 30(suppl. 1):82–90. doi: 10.1159/000341681; pmid: 23075874. [PubMed: 23075874]

47. Powell N, et al. The transcription factor T-bet regulates intestinal inflammation mediated by interleukin-7 $receptor^+$ innate lymphoid cells. Immunity. 2012; 37:674–684. doi: 10.1016/j.immuni.2012.09.008; pmid: 23063332. [PubMed: 23063332]

48. Bruchard M, et al. The receptor NLRP3 is a transcriptional regulator of T_H2 differentiation. Nat. Immunol. 2015; 16:859–870. doi: 10.1038/ni.3202; pmid: 26098997. [PubMed: 26098997]

49. Strainic MG, et al. Locally produced complement fragments C5a and C3a provide both costimulatory and survival signals to naive $CD4^+$ T cells. Immunity. 2008; 28:425–435. doi: 10.1016/j.immuni.2008.02.001; pmid: 18328742. [PubMed: 18328742]
50. Dunkelberger J, Zhou L, Miwa T, Song WC. C5aR expression in a novel GFP reporter gene knockin mouse: Implications for the mechanism of action of C5aR signaling in T cell immunity. J. Immunol. 2012; 188:4032–4042. doi: 10.4049/jimmunol.1103141; pmid: 22430734. [PubMed: 22430734]
51. Karsten CM, et al. Monitoring and cell-specific deletion of C5aR1 using a novel floxed GFP-C5aR1 reporter knock-in mouse. J. Immunol. 2015; 194:1841–1855. pmid: 25589074. [PubMed: 25589074]
52. Kolev M, Le Friec G, Kemper C. Complement—tapping into new sites and effector systems. Nat. Rev. Immunol. 2014; 14:811–820. doi: 10.1038/nri3761; pmid: 25394942. [PubMed: 25394942]
53. Doitsh G, et al. Cell death by pyroptosis drives CD4 T-cell depletion in HIV-1 infection. Nature. 2014; 505:509–514. doi: 10.1038/nature12940; pmid: 24356306. [PubMed: 24356306]
54. Ben-Sasson SZ, et al. IL-1 enhances expansion, effector function, tissue localization, and memory response of antigen-specific CD8 T cells. J. Exp. Med. 2013; 210:491–502. doi: 10.1084/jem.20122006; pmid: 23460726. [PubMed: 23460726]
55. Mayer-Barber KD, et al. Host-directed therapy of tuberculosis based on interleukin-1 and type I interferon crosstalk. Nature. 2014; 511:99–103. doi: 10.1038/nature13489; pmid: 24990750. [PubMed: 24990750]
56. Rasheed MA, et al. Interleukin-21 is a critical cytokine for the generation of virus-specific long-lived plasma cells. J. Virol. 2013; 87:7737–7746. doi: 10.1128/JVI.00063-13; pmid: 23637417. [PubMed: 23637417]
57. Valatas V, et al. Host-dependent control of early regulatory and effector T-cell differentiation underlies the genetic susceptibility of RAG2-deficient mouse strains to transfer colitis. Mucosal Immunol. 2013; 6:601–611. doi: 10.1038/mi.2012.102; pmid: 23149660. [PubMed: 23149660]
58. Bock D, et al. The C terminus of the human C5a receptor (CD88) is required for normal ligand-dependent receptor internalization. Eur. J. Immunol. 1997; 27:1522–1529. doi: 10.1002/eji.1830270631; pmid: 9209506. [PubMed: 9209506]
59. Subramanian A, et al. Gene set enrichment analysis: A knowledge-based approach for interpreting genome-wide expression profiles. Proc. Natl. Acad. Sci. U.S.A. 2005; 102:15545–15550. doi: 10.1073/pnas.0506580102; pmid: 16199517. [PubMed: 16199517]

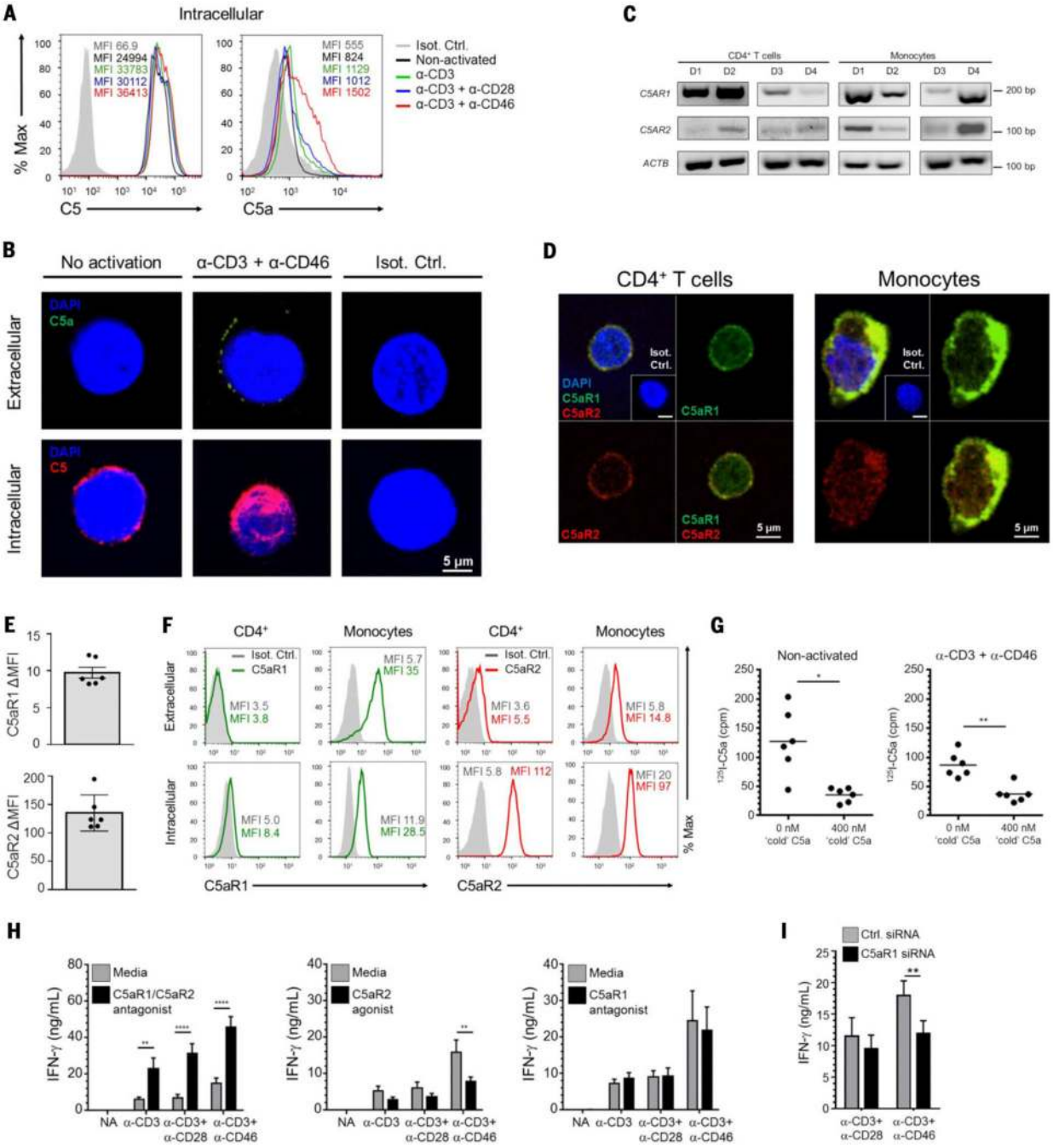

Fig. 1. Autocrine activation of C5a receptors regulates IFN-γ production by human CD4$^+$ T cells

(**A** and **B**) Intracellular C5 and C5a generation in CD4$^+$ T lymphocytes, left nonactivated or activated (36 hours) with anti-CD3 (α-CD3), α-CD3 + α-CD28, or α-CD3 + α-CD46 by flow cytometry (A) and confocal microscopy (B) (data representative of $n = 3$). (**C**) RT-PCR analysis for *C5AR1* and *C5AR2* mRNA in resting human CD4$^+$ cells and monocytes ($n = 4$, donors D1 to D4, endogenous control *ACTB*). (*D*) Intracellular immunofluorescence on resting T cells and monocytes with antibodies to C5aR1 (green) and C5aR2 (red) (data are representative of $n = 3$). (**E**) C5aR1 and C5aR2 protein amounts in T cells with expression

normalized to respective isotype control staining for each donor (change in mean fluorescence intensity ΔMFI ± SEM, $n = 6$). (*F*) Flow cytometry for C5aR1 and C5aR2 on resting T cells and monocytes, with representative histogram plots shown ($n = 6$). (**G**) Binding of radioactively labeled ^{125}I-C5a in absence or presence of nonlabeled "cold" C5a as competitor to resting or α-CD3 + α-CD46 activated (4 hours) T cells ($n = 6$). (**H**) IFN-γ secretion in nonactivated (NA) and activated (36 hours) $CD4^+$ T cells in the absence or presence of a C5aR1/C5aR2 double receptor antagonist ($n = 9$), a C5aR2 agonist ($n = 8$), or a C5aR1 antagonist ($n = 7$). (I) IFN-γ production by T cells transfected with C5aR1-specific siRNA or a scrambled control siRNA (Ctrl. siRNA) 36 hours after activation ($n = 7$). Data are means ± SEM. $^*P < 0.05$, $^{**}P < 0.01$, $^{****}P < 0.0001$. (G), paired *t* test; (H) and (I), two-way ANOVA with Bonferroni multiple comparison test.

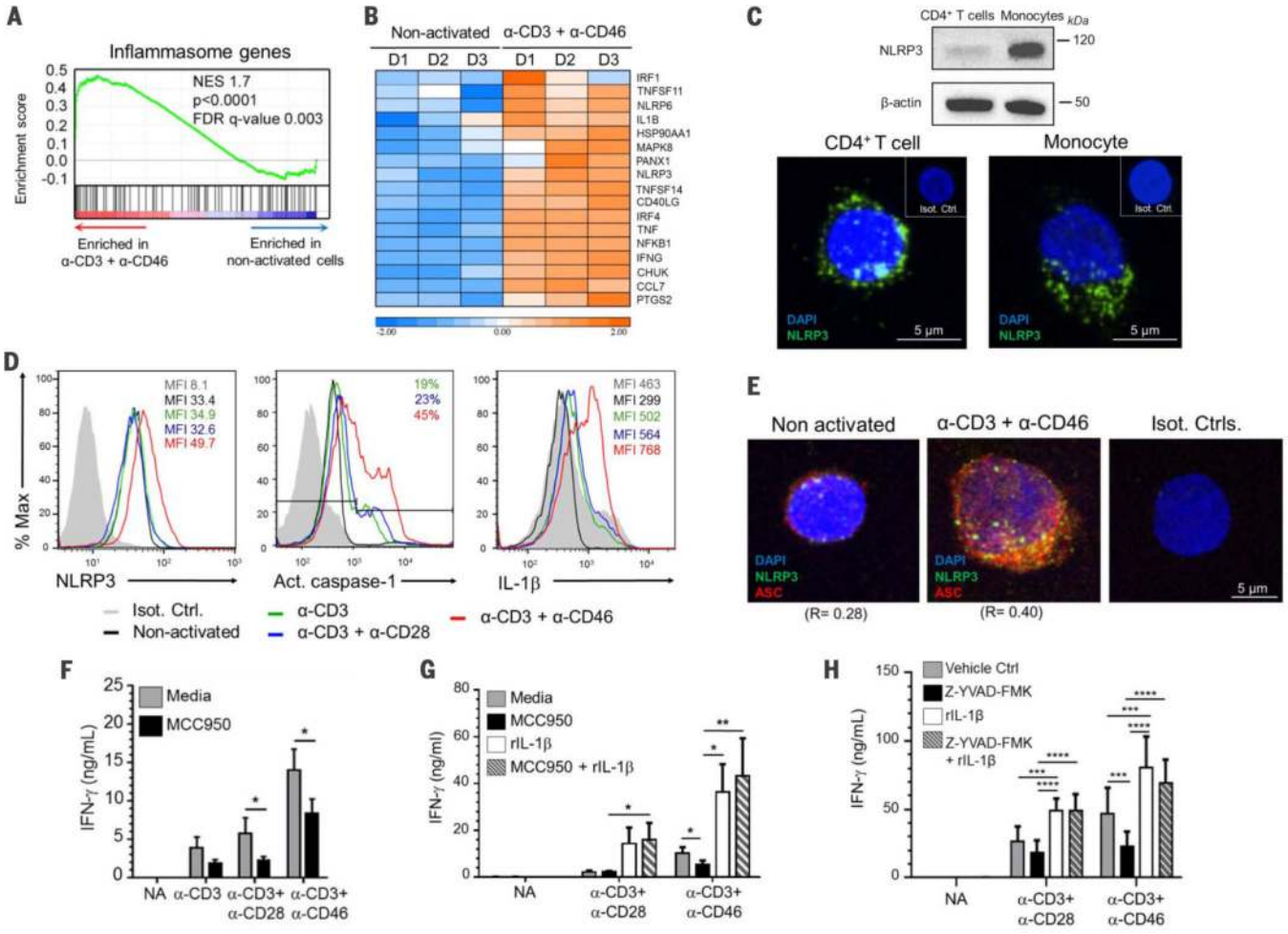

Fig. 2. NLRP3 inflammasome activation occurs in CD4$^+$ T cells and enhances IFN-γ production

(**A**) Gene set enrichment analysis (GSEA) for inflammasome-related genes in CD4$^+$ T cells after α-CD3 + α-CD46 activation (2 hours) compared to resting cells (donors D1 to D3). (**B**) Heat map depicting leading edge analysis (the core enriched genes) of the data in (A). (**C**) NLRP3 immunoblot (upper panel) and immunofluorescence (lower panel) on CD4$^+$ lymphocytes and monocytes (data representative of $n = 3$). (**D**) NLRP3, activated caspase-1 and total IL-1β protein expression in activated CD4$^+$ cells (data representative of $n = 3$). (**E**) Representative immunofluorescence costaining for NLRP3 (green) and ASC (red) on resting and α-CD3 + α-CD46 activated T cells (r = Pearson correlation coefficient between NLRP3 and ASC fluorescence, $n = 3$). (**F** and **G**) IFN-γ production by resting (NA) and activated CD4$^+$ T cells with or without MCC950 addition ($n = 7$) (F) and with or without rhIL-1β supplementation ($n = 3$) (G). (**H**) IFN-γ production in presence of the specific caspase-1 inhibitor Z-YVAD-FMK with or without rhIL-1β addition. *$P < 0.05$, **$P < 0.01$, ***$P < 0.001$, ****$P < 0.0001$. (F) to (H), two-way ANOVA with Bonferroni multiple comparison test.

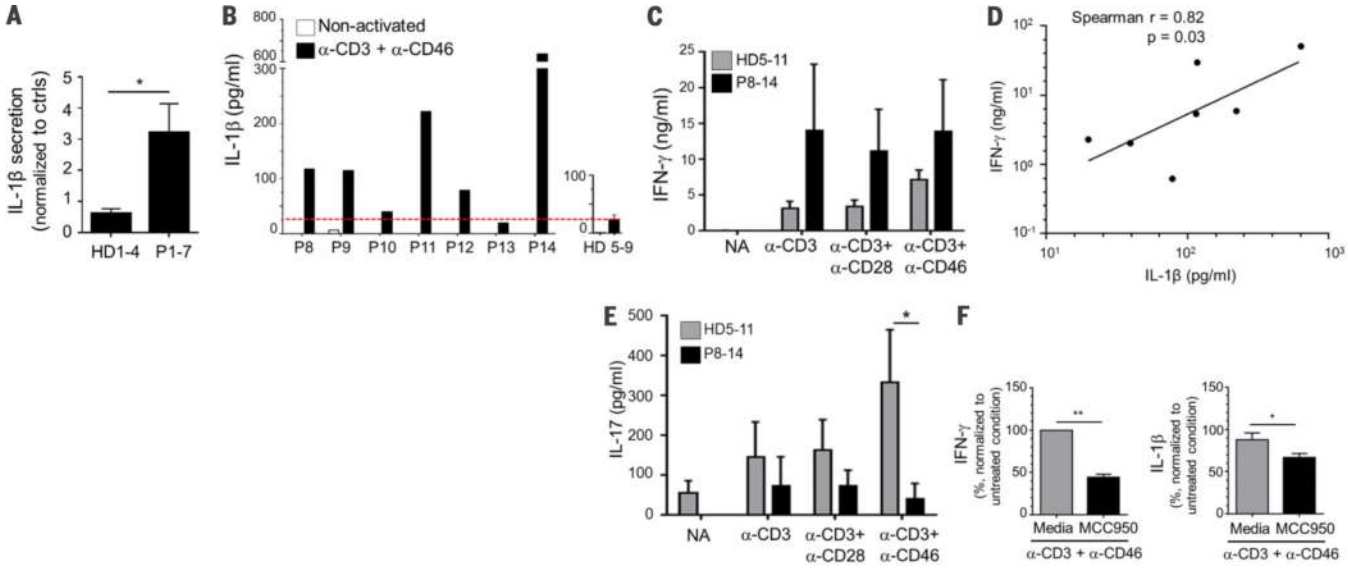

Fig. 3. T cells from CAPS patients have increased NLRP3 inflammasome activity and hyperactive T_H1 responses

(**A**) IL-1β production from $CD4^+$ T cells activated with α-CD3 + α-CD46 for 36 hours from four healthy donors (HD1 to HD4) and seven patients with CAPS (cohort 1, P1 to P7). (**B**) IL-1β secretion from resting and α-CD3 + α-CD46 activated $CD4^+$ cells from seven patients with CAPS (P8 to P14, individual values) and five healthy sex- and age-matched donors (HD5 to HD9, combined values). (**C**) IFN-γ secretion from resting and activated $CD4^+$ cells from seven patients with CAPS (P8 to P14) and seven healthy sex- and age-matched donors (HD5 to HD11). (**D**) Correlation between IL-1β and IFN-γ production in T cells from patients P8 to P14 upon α-CD3 + α-CD46 activation (Spearman correlation analysis). (**E**) IL-17 production by resting and activated T cells from CAPS patients P8 to P14 and healthy donors H5 to H11. (**F**) IFN-γ and IL-1β secretion by $CD4^+$ T cells from P8, P11, and P14 after α-CD3 + α-CD46 activation with or without MCC950 treatment (% normalized to nontreated). Analyses on (A) to (F) were performed at 36 hours after activation. Values correspond to two technical replicates for every patient and healthy control sample in each experiment. Data are means ± SEM. $*P < 0.05$, $**P < 0.01$. (A), unpaired *t* test; (C) and (E), two-way ANOVA with Bonferroni multiple comparison test; (D), Spearman correlation test; (F), paired *t* test.

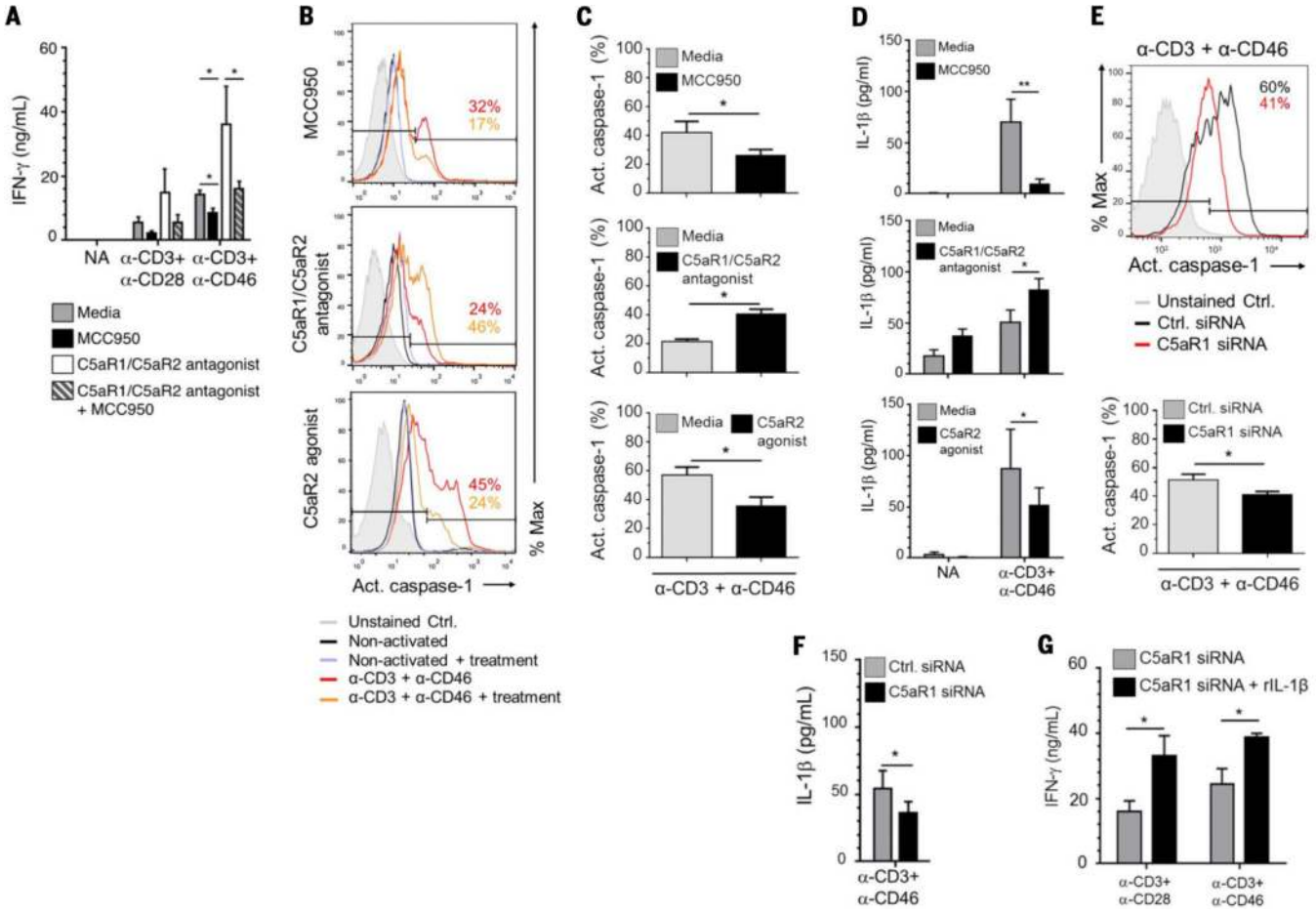

Fig. 4. C5a receptors modulate NLRP3 activation to regulate IFN-γ responses

(**A**) IFN-γ production in CD4$^+$ T cells either left nonactivated (NA) or activated as depicted with or without addition of the C5aR1/C5aR2 antagonist and/or MCC950 ($n = 3$). (**B** and **C**) Measurement of active caspase-1–positive CD4$^+$ T cells activated with α-CD3 + α-CD46 with or without MCC950, the C5aR1/C5aR2 antagonist or the C5aR2 agonist ($n = 3$) (B) and statistical analyses of data obtained (C). (**D**) Corresponding IL-1β secretion in activated CD4$^+$ cells treated as in (B) ($n = 5$). (**E** and **F**) Active caspase-1 levels [(E), $n = 4$] and IL-1β secretion [(F), $n = 7$] in T cells after transfection with either C5aR1-specific siRNA or scrambled control (Ctrl.) siRNA. (**G**) IFN-γ production in activated CD4$^+$ T cells after transfection with C5aR1-specific siRNA or a scrambled control siRNA (Ctrl. siRNA) with or without addition of rhIL-1β ($n = 3$). Analyses were performed at 36 hours after activation. Data are means ± SEM. *$P < 0.05$, **$P < 0.01$. (A), (D), and (G), two-way ANOVA with Bonferroni multiple comparison test; (C), (E), and (F), paired *t* test.

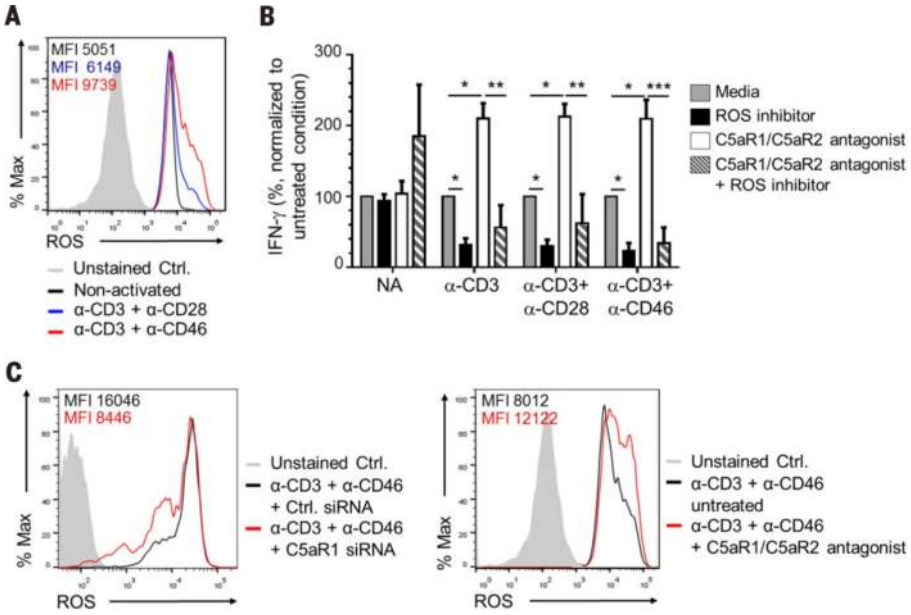

Fig. 5. Intracellular C5aR1 activation induces ROS generation in CD4$^+$ T cells

(**A**) ROS production in CD4$^+$ T cells activated under the depicted conditions (data shown are representative of $n = 3$). (**B**) IFN-γ production from CD4$^+$ T cells left nonactivated or activated as indicated with and without a specific ROS inhibitor and/or the C5aR1/C5aR2 antagonist ($n = 3$). Data are from a two-way ANOVA with Bonferroni multiple comparison test. (**C**) ROS production in α-CD3 + α-CD46 activated CD4$^+$ cells after transfection with C5aR1-specific siRNA (left panel) or with or without the C5aR1/C5aR2 double antagonist (right panel) (data shown are representative of $n = 3$). Analyses were performed 36 hours after activation. Data are means ± SEM. *$P < 0.05$, **$P < 0.01$, ***$P < 0.001$.

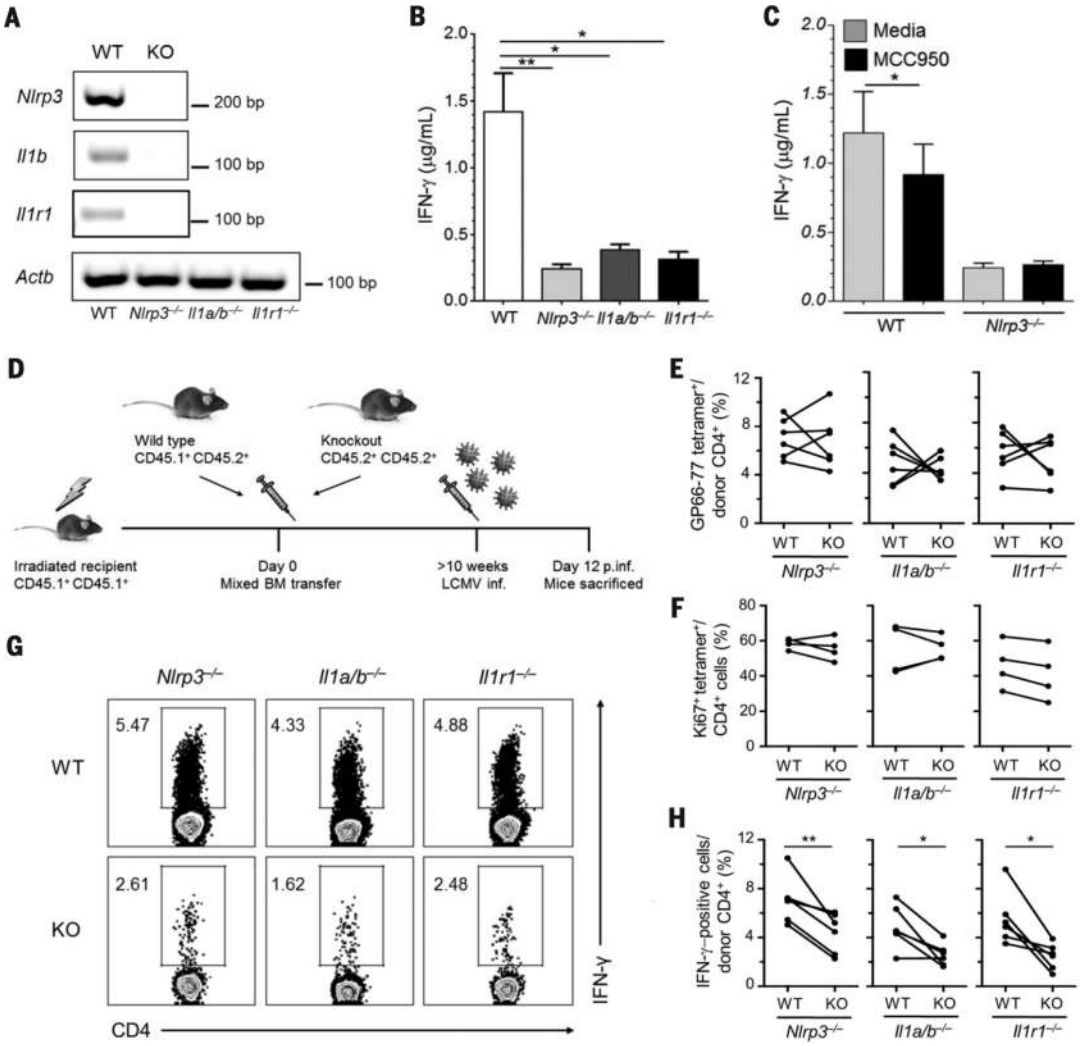

Fig. 6. NLRP3 function in CD4$^+$ T cells drives optimal IFN-γ production during viral infection

(**A**) RT-PCR analysis on CD4$^+$ T cells isolated from wild type (WT), *Nlrp3*$^{-}$, combined *Il1a*$^{-/-}$ and *Il1b*$^{-/-}$ (*Il1a/b*$^{-/-}$) and *Il1r1*$^{-/-}$ mice for corresponding gene mRNA expression. (**B**) Cytokine secretion from CD4$^+$ T cells isolated from wild-type and knockout mice at 96 hours after α-CD3 + α-CD28 activation ($n = 3$). (**C**) Cytokine production from CD4$^+$ T cells from wild-type and *Nlrp3*$^{-/-}$ mice after α-CD3 + α-CD28 activation (96 hours) with or without addition of MCC950 ($n = 4$). (**D**) Schematic of the acute lymphocytic choriomeningitis virus (LCMV) infection model used in this study. (**E** and **F**) Percentage of LCMV tetramer-positive CD4$^+$ T cells isolated from the spleens of the three bone marrow chimeric mice groups used 12 days after infection (E) and percentages of Ki67$^+$GP66-77$^+$/ tetramer-positive cells (F). (**G** and **H**) Representative intracellular IFN-γ staining in splenic CD4$^+$ T cells of one mouse from each group after LCMV peptide restimulation (5 hours) [(G), $n = 6$] with corresponding statistical analyses [(H), $n = 6$]. Data are means ± SEM. *$P < 0.05$, **$P < 0.01$. (B), one-way ANOVA with Tukey multiple comparison test; (C), two-way ANOVA with Bonferroni multiple comparison test; (E) to (H), paired *t* test. Data in (G)

are representative of two independent experiments; data in (E), (F), and (H) are pooled from two independent experiments.

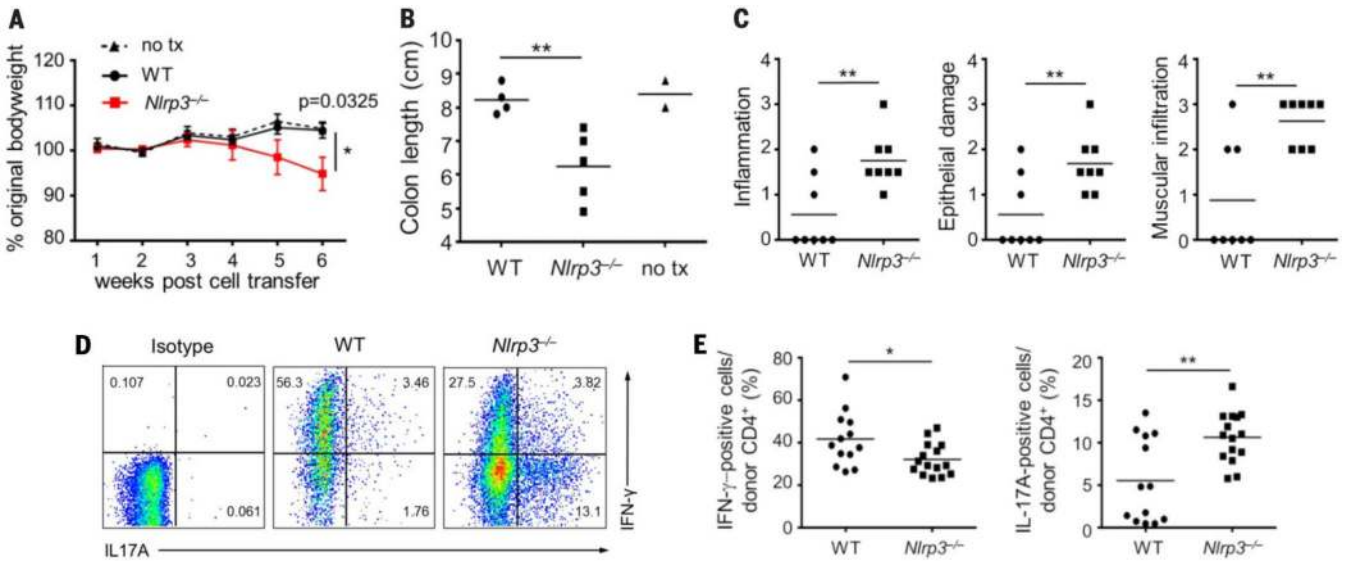

Fig. 7. T cell intrinsic NLRP3 activity regulates the T_H1-T_H17 balance in intestinal inflammation

(**A** to **E**) Naïve splenic CD25$^-$CD45RB^{hi} CD4$^+$ T cells from wild-type or *Nlpr3*$^{-/-}$ mice were transferred into C57BL/10 *Rag2*$^{-/-}$ mice. (**A**) Weight change over the course of colitis induction. (**B**) Colon length at the study endpoint. (**C**) Inflammation score of the colons according to blinded histological analysis with assessment of inflammation (left panel), epithelial damage (middle panel) and muscular immune cell infiltration (right panel). (**D** and **E**) Intracellular IFN-γ and IL-17A staining of colonic CD4$^+$ T cells at the study endpoint after overnight α-CD3 + α-CD28 stimulation and brefeldin A and monensin addition for 5 hours (gated on live CD4$^+$ Thy1.2$^+$ T cells). Representative flow cytometric plots (D) with corresponding statistical analysis shown from two combined independent experiments [(E), $n = 13$ wild-type, $n = 15$ KO]. Data are means ± SEM. $^*P < 0.05$, $^{**}P < 0.01$. (A) and (B), one-way ANOVA with Sidak multiple-comparisons test; (C) and (E), unpaired *t* test. Data are representative of two experiments [(A) to (C)] or are combined from two experiments (E).